ESI:

Electronic Modulation of Composite Electrocatalysts Derived from Layered NiFeMn Triple Hydroxide Nanosheets for Boosted Overall Water Splitting

Lei Yan,[‡a] Yanrong Ren,[‡a] Xiaolong Zhang,[‡b] Yulin Sun,[a] Jiqiang Ning,[c] Yijun Zhong,[a] Botao Teng[a] and Yong Hu*[a]

[a]Key Laboratory of the Ministry of Education for Advanced Catalysis Materials, Department of Chemistry, Zhejiang Normal University, Jinhua 321004, China. E-mail: yonghu@zjnu.edu.cn; yonghuzjnu@163.com

[b]Division of Nanomaterials & Chemistry, Hefei National Research Center for Physical Sciences at the Microscale, CAS Center for Excellence in Nanoscience, Hefei Science Center of CAS, Collaborative Innovation Center of Suzhou Nano Science and Technology, Department of Chemistry, University of Science and Technology of China, Hefei 230026, China.

[c]Vacuum Interconnected Nanotech Workstation, Suzhou Institute of Nano-Tech and Nano-Bionics, Chinese Academy of Sciences, Suzhou 215123, China.

[†]Electronic supplementary information (ESI) available. See DOI: https://pubs.rsc.org/

[‡] These authors contributed equally to this work.
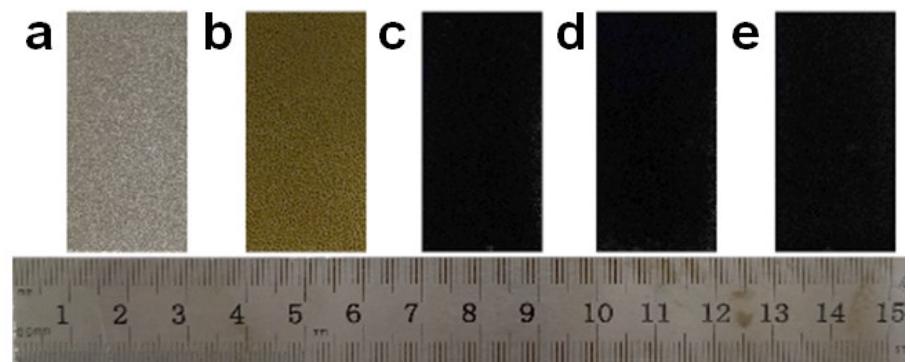
Fig. S1 Photograph of (a) NF, (b) NiFeMn-LTH/NF, (c) NiFeMn-LTH/FM-NS/NF-4, (d) NiFeMn-LTH/FM-NS/NF-8, (e) FM-NS/NF electrodes.
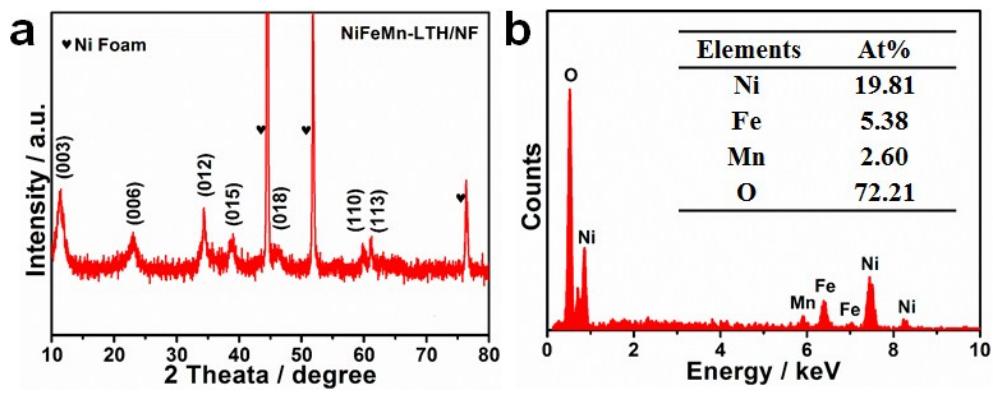
**Fig. S2** (a) XRD pattern and (b) EDS spectrum of the as-prepared NiFeMn-LTH NSAs.
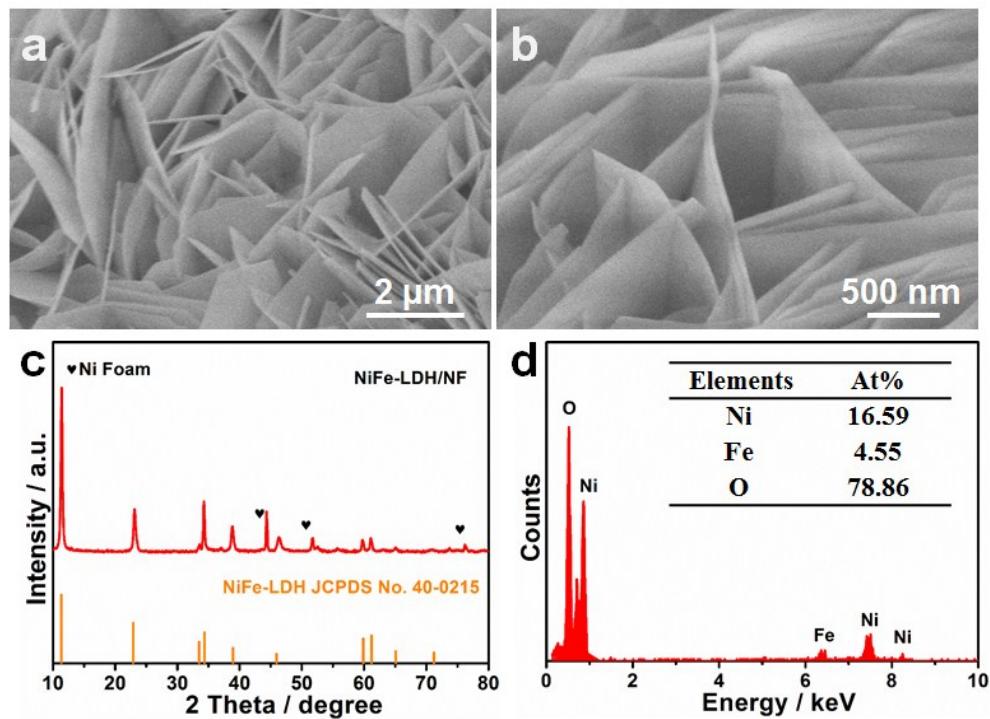
Fig. S3 (a, b) SEM images, (c) XRD pattern and (d) EDS spectrum of the as-obtained NiFe-LDH

NSAs.
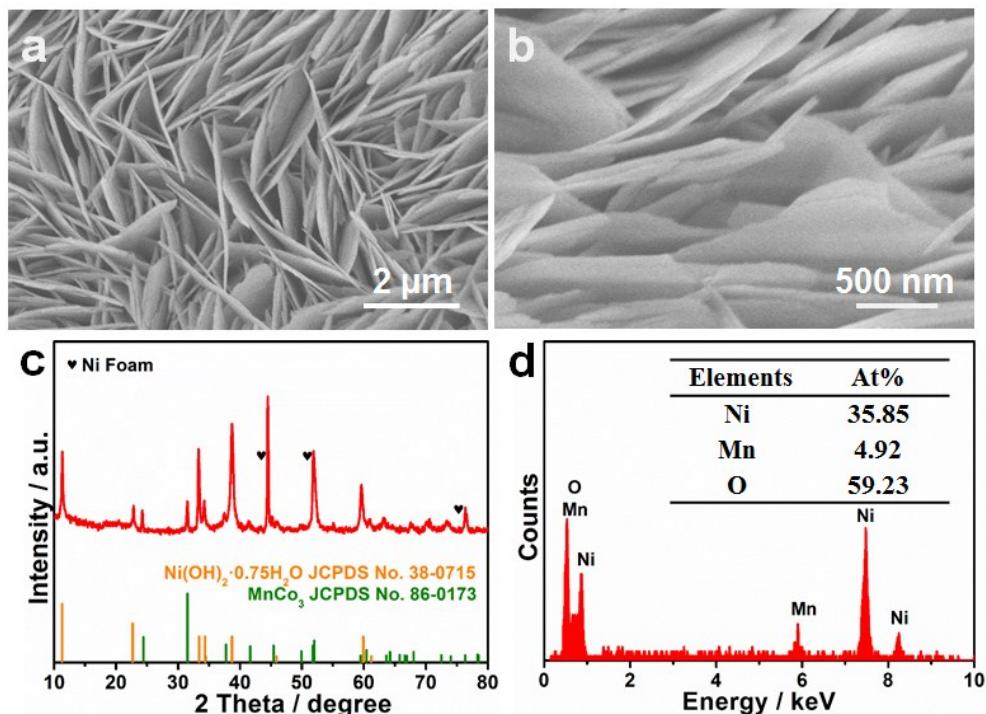
**Fig. S4** (a, b) SEM images, (c) XRD patterns and (d) EDS spectrum of the as-prepared Ni-Mn precursor NSAs.
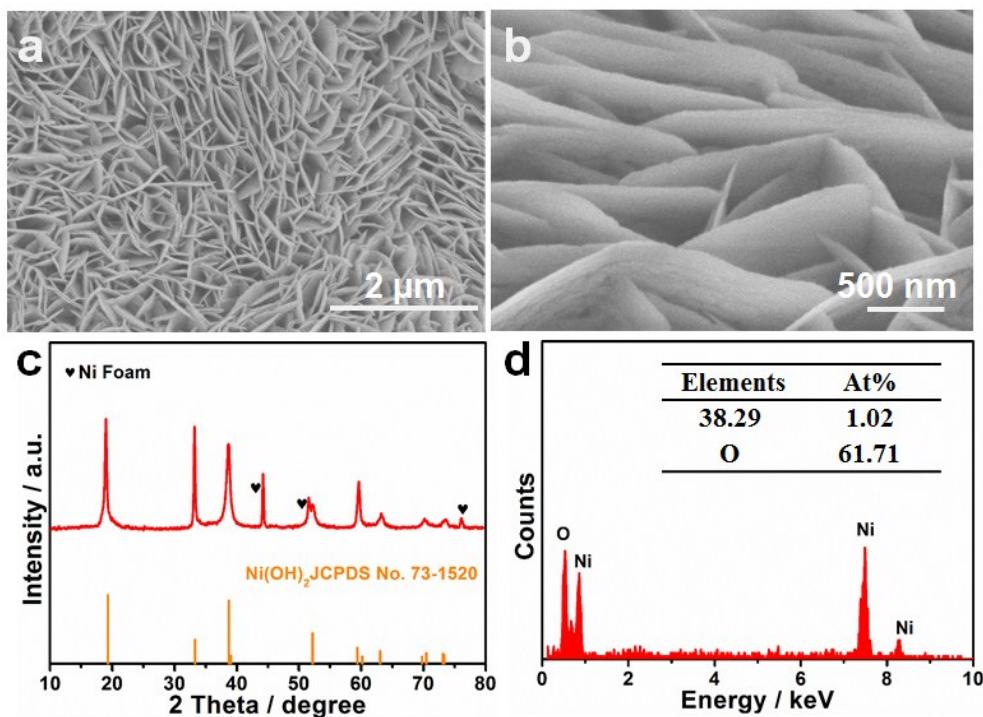
**Fig. S5** (a, b) SEM images, (c) XRD pattern and (d) EDS spectrum of the as-prepared Ni(OH)$_2$ NSAs.
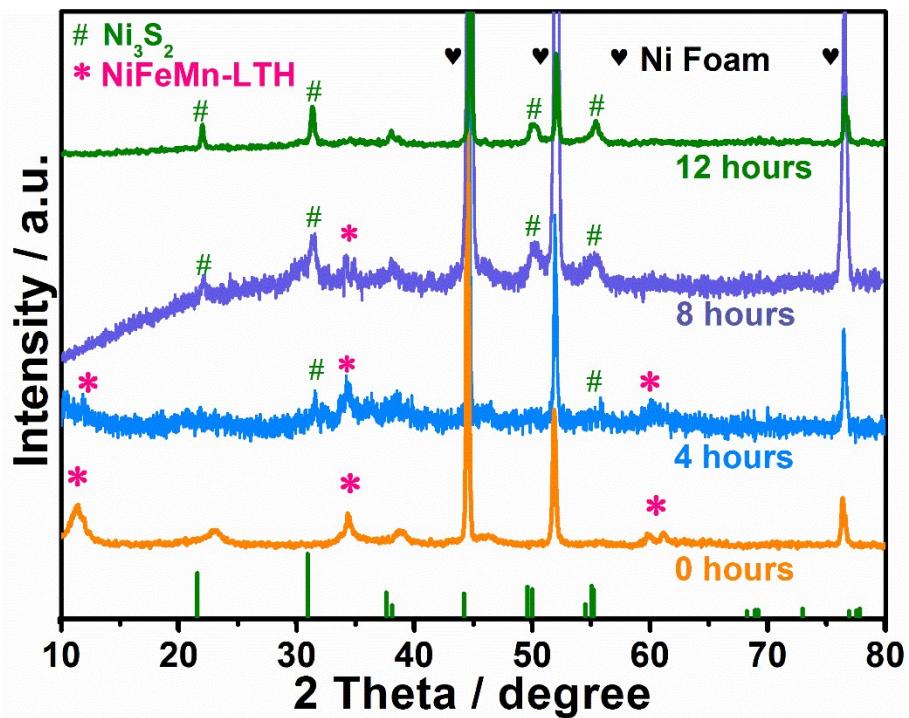
Fig. S6 XRD patterns of the as-prepared NiFeMn-LDH, NiFeMn-LTH/FM-NS-4 HNSAs, NiFeMn-LTH/FM-NS-8 HNSAs and FM-NS NSAs.
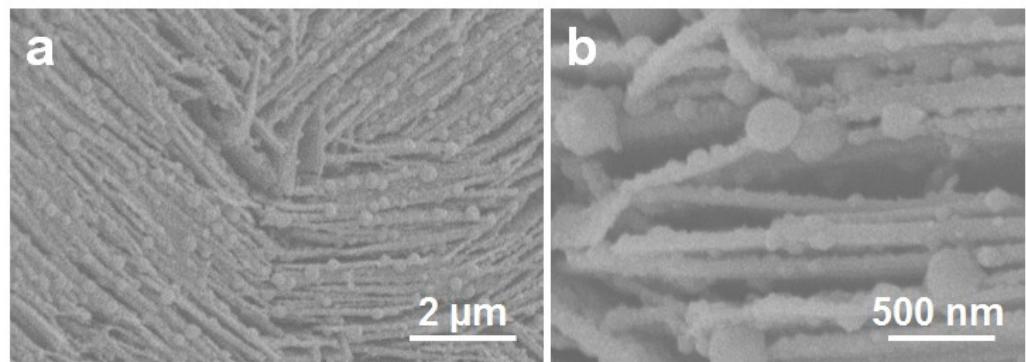
Fig. S7 (a, b) SEM images of the as-prepared NiFeMn-LTH/FM-NS/NF-8 NSAs.
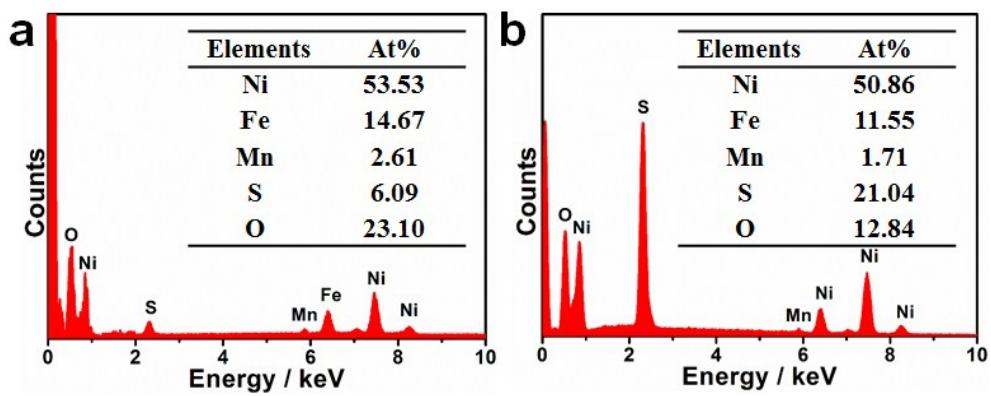
**Fig. S8** (a) EDS spctra of the as-prepared NiFeMn-LTH/FM-NS-4 HNSAs and (b) FM-NS NSAs.
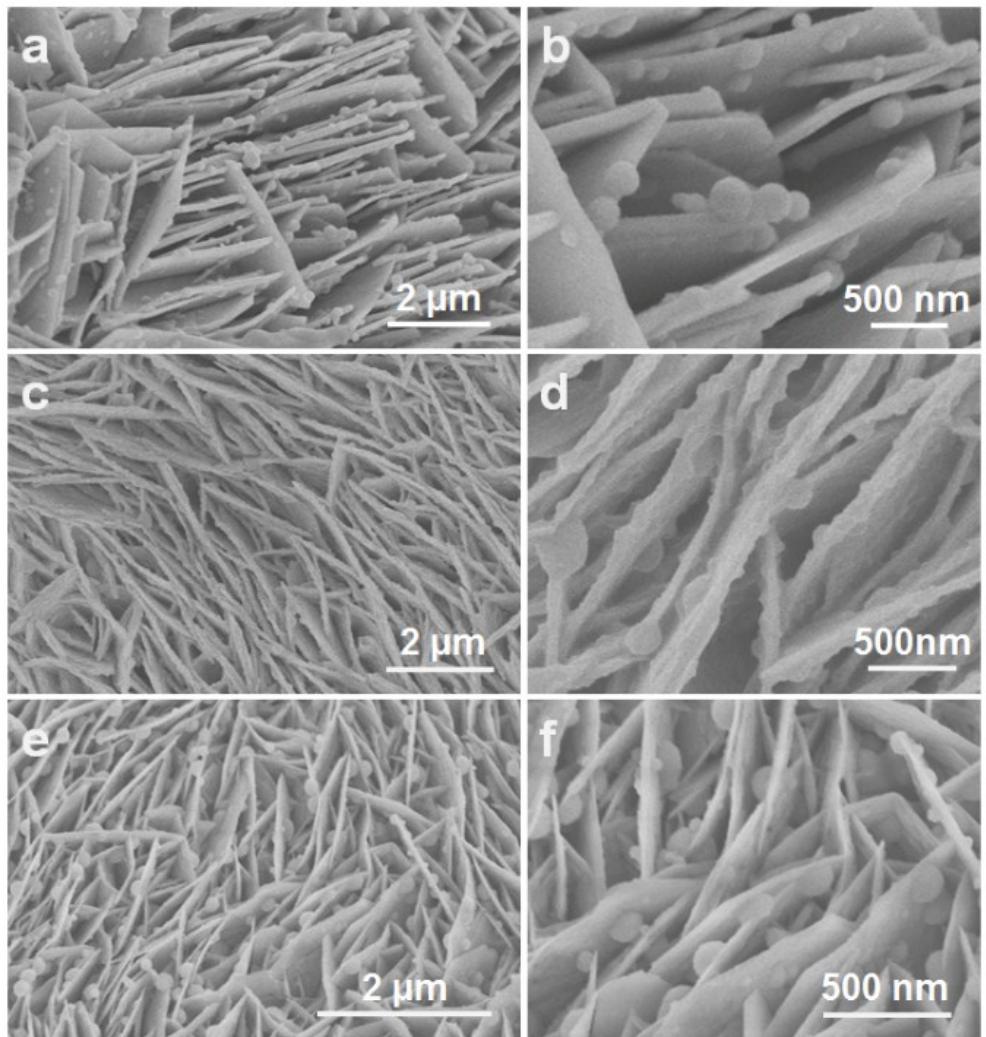
Fig. S9 (a, b) SEM images of the as-prepared Fe-NS, (c, d) Mn-NS and (e, f) NS NSAs.
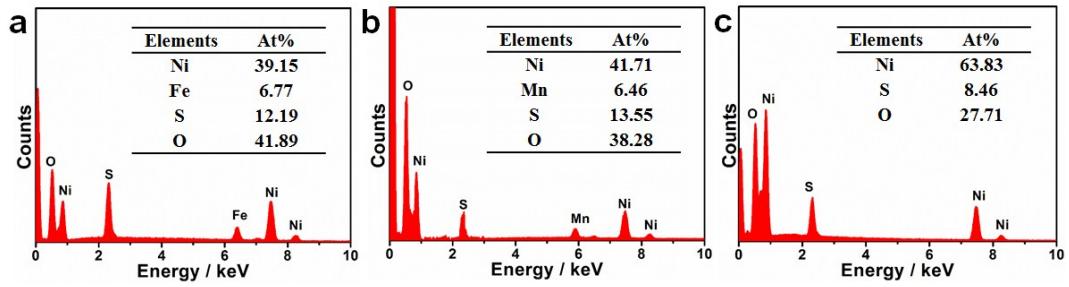
Fig. S10 (a) EDS spectra of the as-prepared Fe-NS, (b) Mn-NS and (c) NS NSAs.
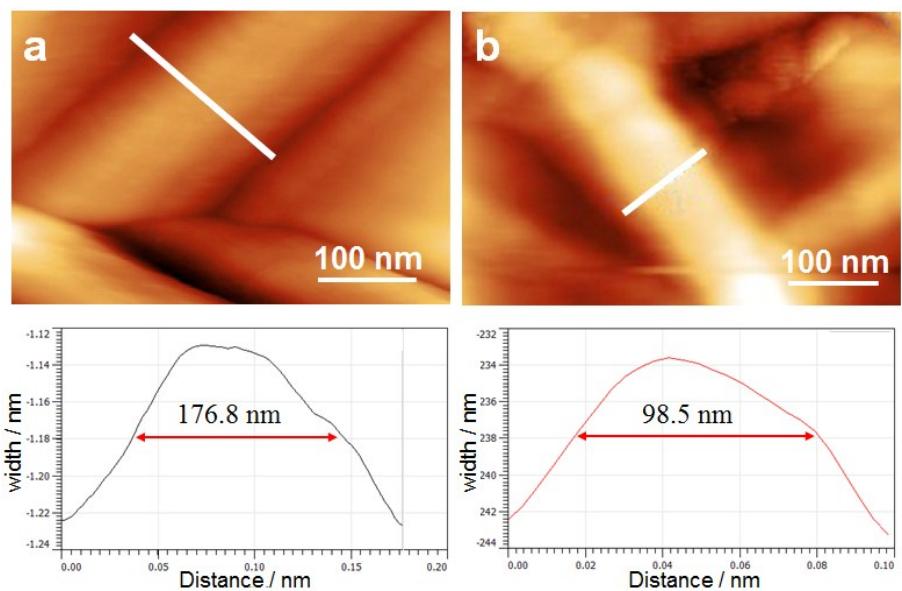
Fig. S11 AFM images and the corresponding width profiles of (a) the FM-NS and (b) NS NSAs.
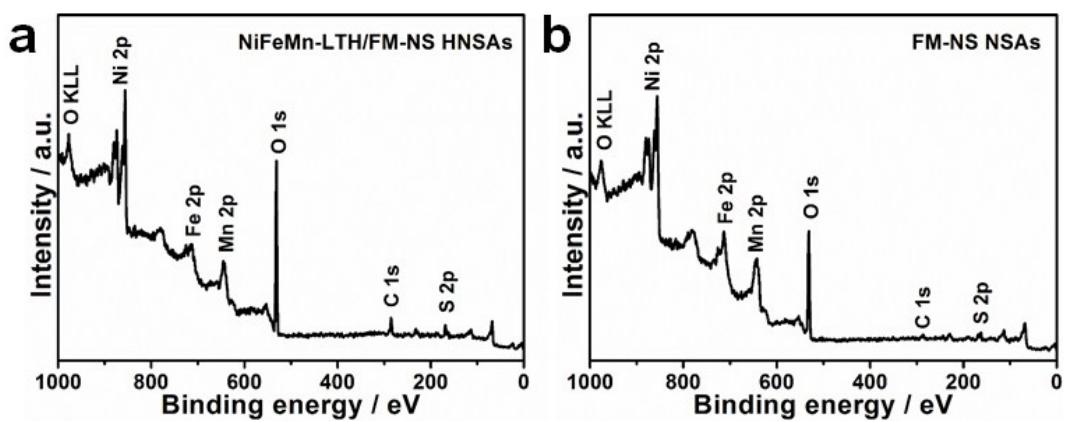
Fig. S12 (a, b) XPS survey spectra of the as-prepared NiFeMn-LTH/FM-NS-4 HNSAs and FM-

NS NSAs. The result reveals that the two are mainly composed of Ni, Fe, Mn and S elements.
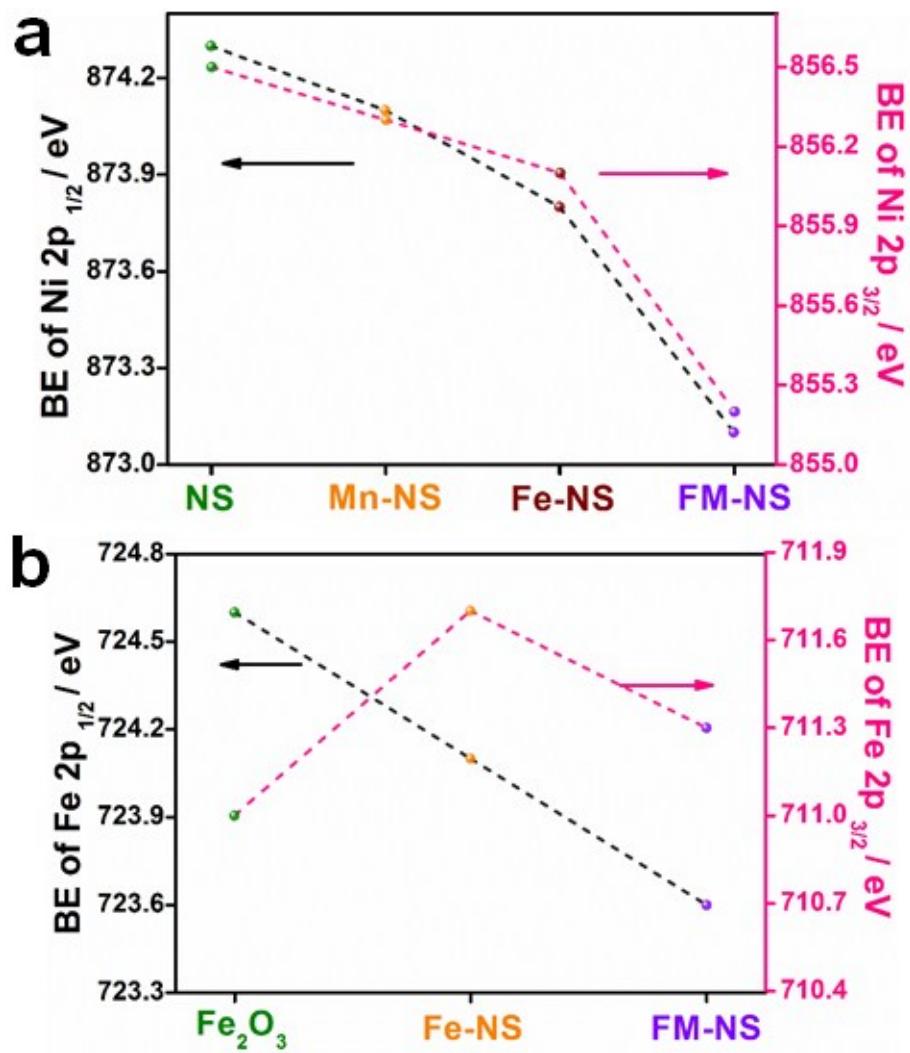
Fig. S13 Changes in binding energy of (a) Ni 2p, (b) Fe 2p for the as-prepared FM-NS, Fe-NS,

Mn-NS and pure NS NSAs catalysts, together with Fe_2O_3 as unary metal oxide references.
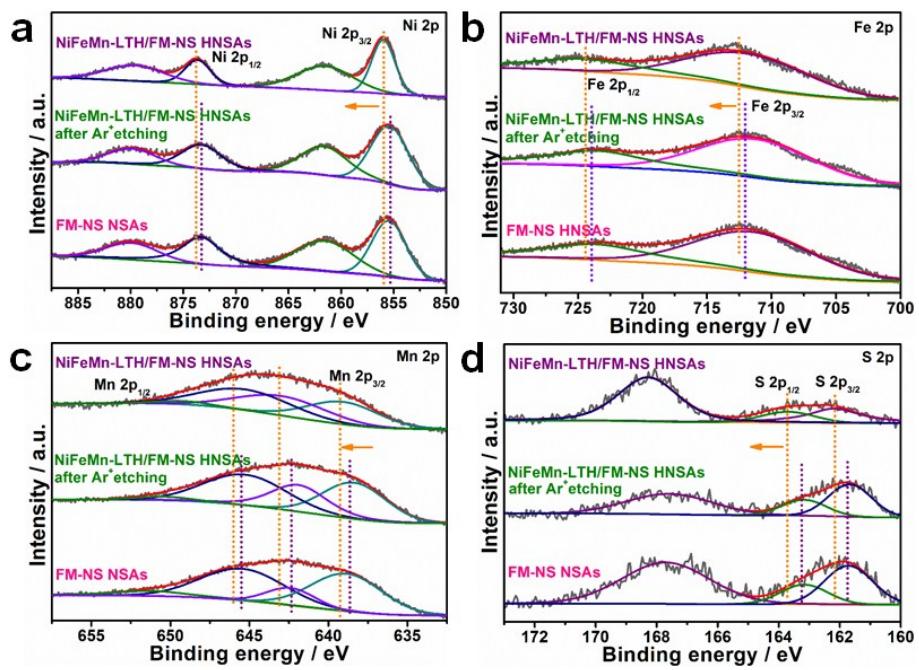
Fig. S14 XPS spectra of (a) Ni 2p, (b) Fe 2p, (c) Mn 2p and (d) S 2p of the as-prepared NiFeMn-

LTH/FM-NS-4 HNSAs before and after 60s Ar$^+$ etching and FM-NS NSAs.
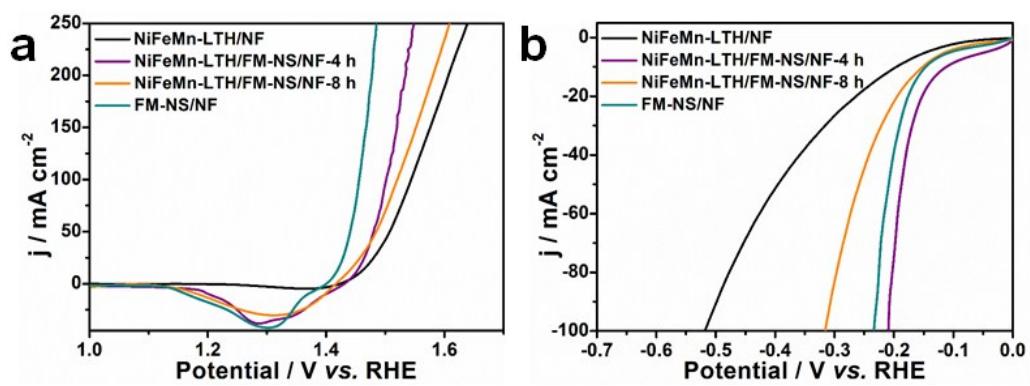
Fig. S15 The LSV curves for (a) OER and (b) HER of the as-prepared NiFeMn-LTH, NiFeMn-LTH/FM-NS/NF-4, NiFeMn-LTH/FM-NS/NF-8 and FM-NS/NF in 1 M KOH.
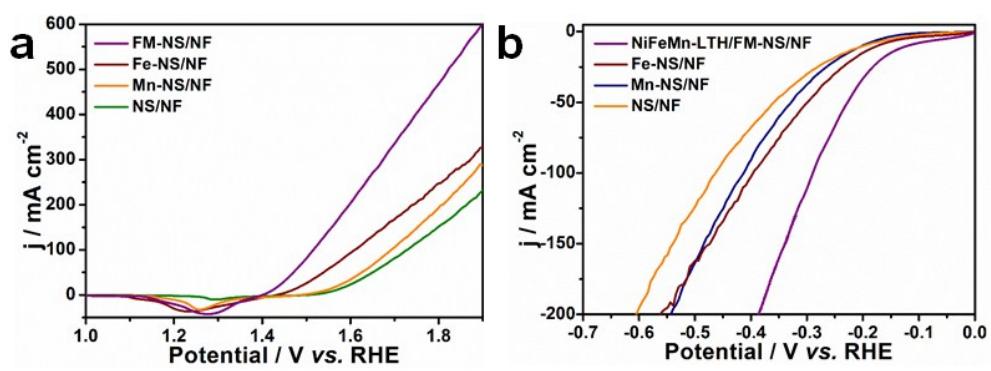
Fig. S16 LSV curves for (a) OER and (b) HER of the as-prepared FM-NS/NF, Fe-NS/NF, Mn-NS/NF, NS/NF and NiFeMn-LTH/FM-NS/NF-4 electrodes in 1 M KOH without iR-corrected.
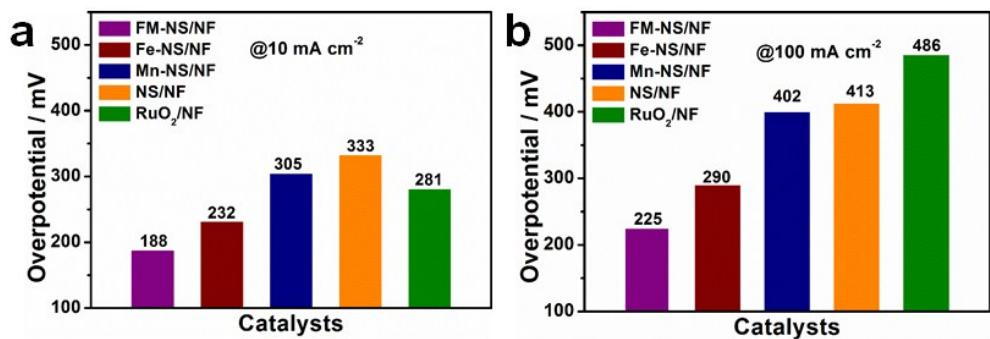
Fig. S17 (a) OER overpotentials required for j=10 mA cm^{-2} and (b) OER overpotentials required for j=100 mA cm^{-2}.
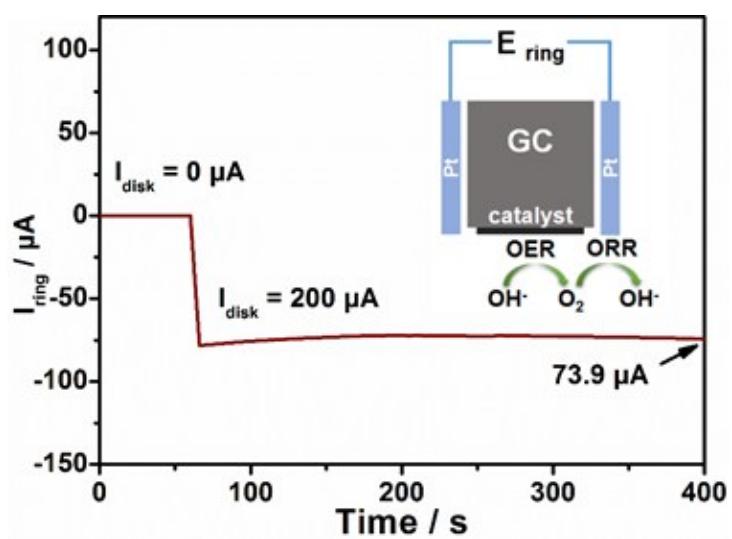
Fig. S18 The ring current recorded on an RRDE setup in 0.1 M KOH solution at room temperature.
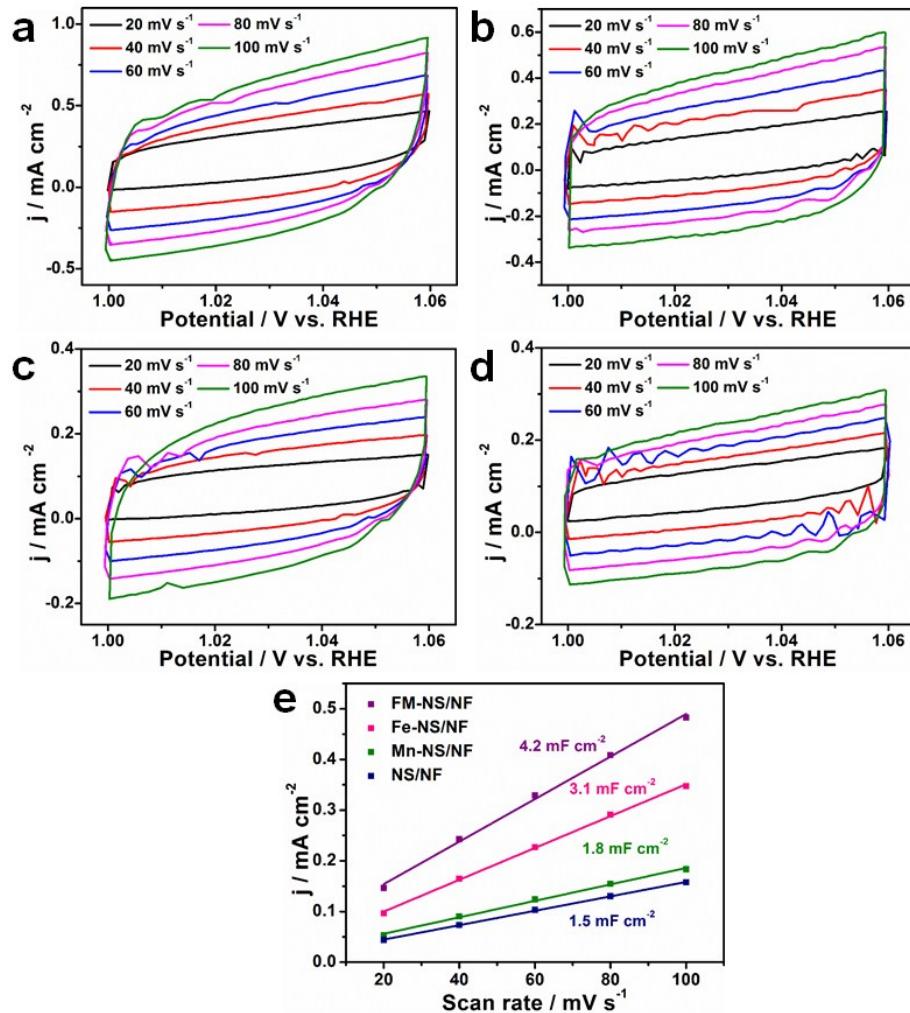
Fig. S19 Electrochemical double-layer capacitance measurements at different scan rate (20, 40, 60, 80, 100 mV s^{-1}) for OER in 1.0 M KOH. Cyclic voltammograms of the as-prepared (a) FM-NS/NF, (b) Fe-NS/NF, (c) Mn-NS/NF, (d) NS/NF electrodes and (e) Charging current density plots with different scan rates for OER. The linear slope, equivalent to twice the double-layer capacitance (C$_{dl}$), was used to represent the ECSA.
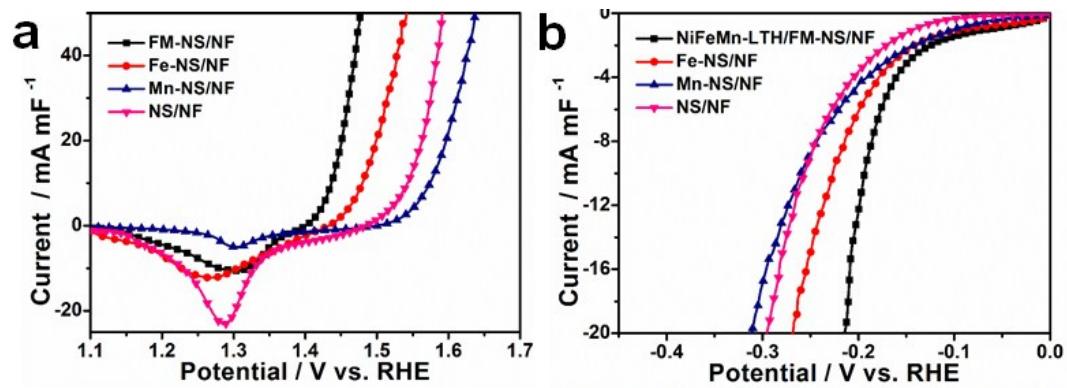
Fig. S20 (a) OER and (b) HER polarization curves normalized by the electrochemical active surface area.
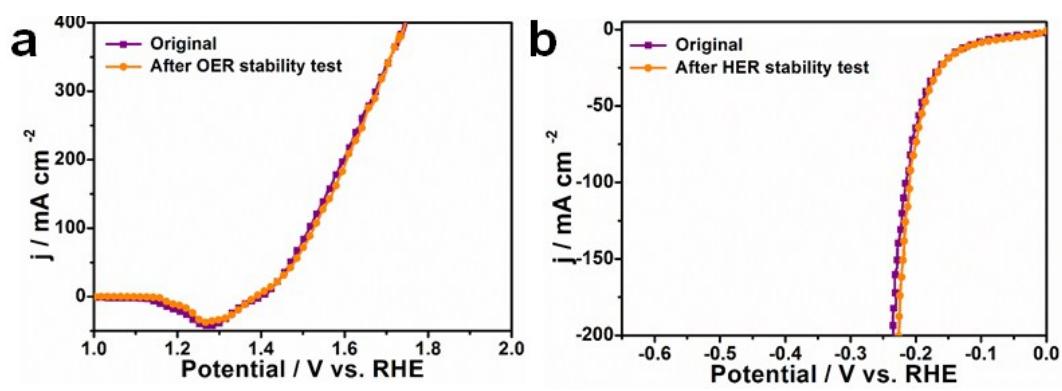
Fig. S21 (a) OER and (b) HER polarization curves before and after 24h stability test.
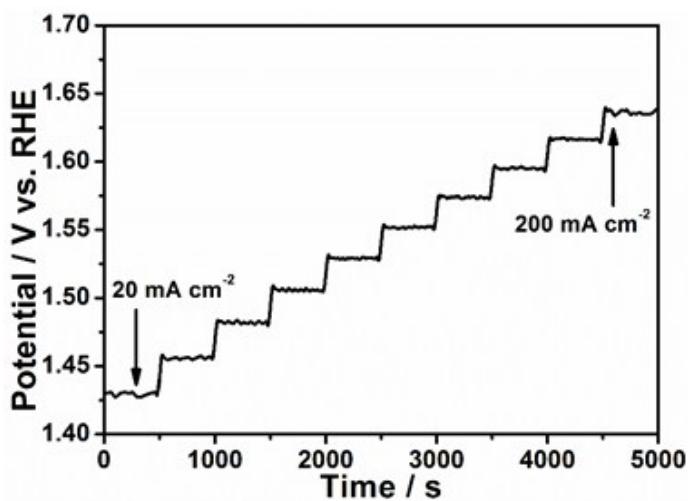
Fig. S22 Multicurrent process of the as-prepared FM-NS/NF electrode for OER. The current density started at 20 mA cm^{-2} and ended at 200 mA cm^{-2}, with an increment of 20 mA cm^{-2} per 500 s without iR correction.
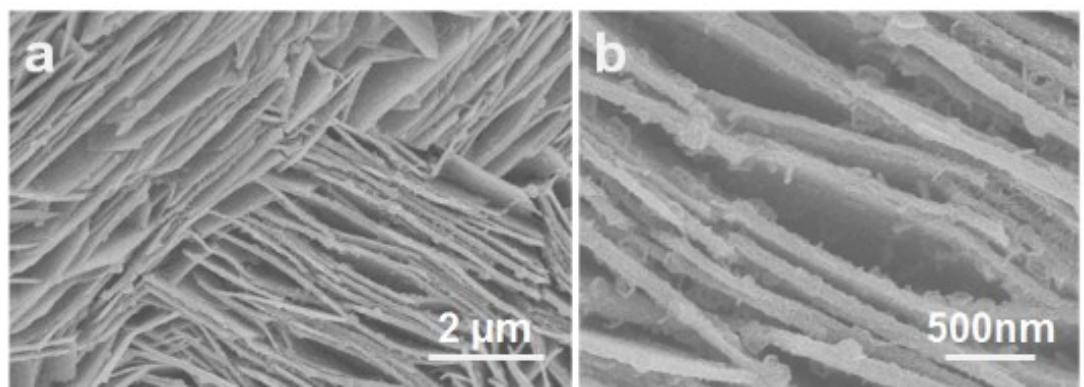
Fig. S23 SEM images of the as-prepared FM-NS/NF electrode after OER test.
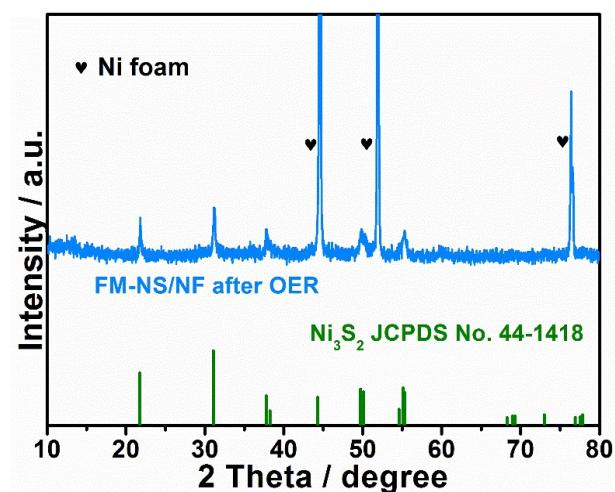
Fig. S24 XRD pattern of the as-prepared FM-NS/NF after OER test.
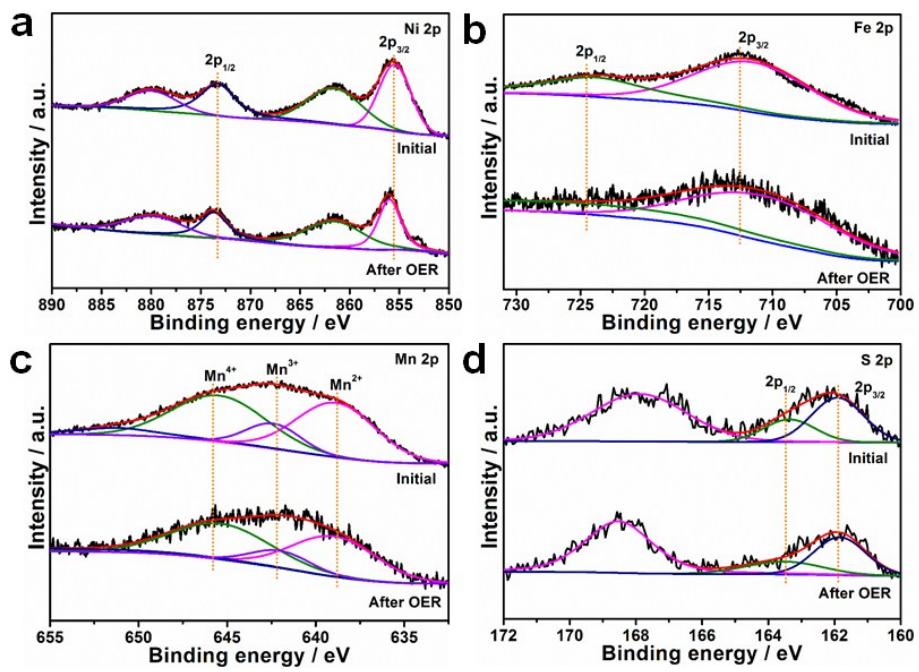
Fig. S25 XPS spectra of (a) Ni 2p, (b) Fe 2p, (c) Mn 2p and (d) S 2p of the as-prepared FM-NS/NF before and after OER test.
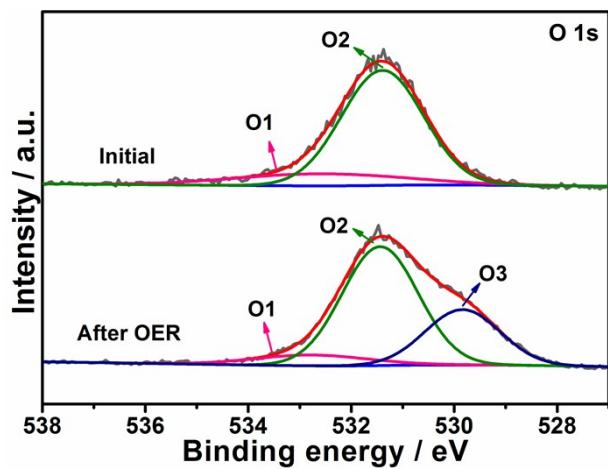
Fig. S26 XPS spectra of O 1s of the as-prepared FM-NS/NF before and after OER test.
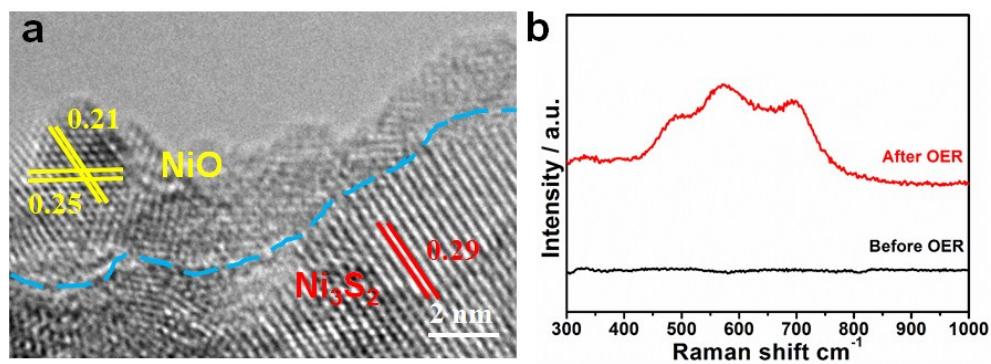
Fig. S27 (a) HRTEM image of the as-prepared FM-NS nanosheet after OER test and (b) Raman of the as-prepared FM-NS/NF before and after OER test.
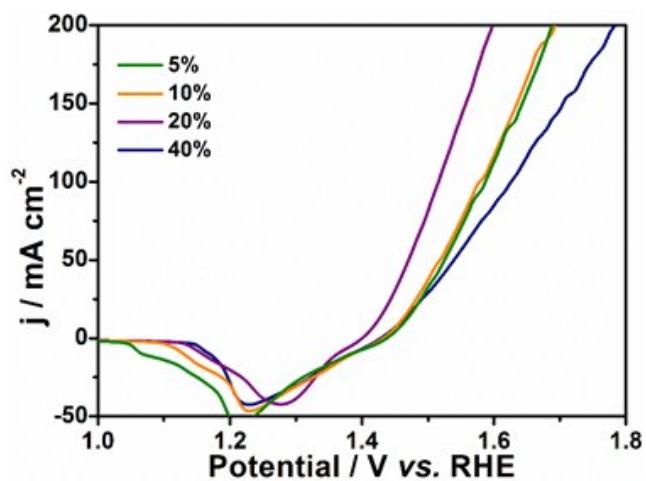
Fig. S28 Linear sweep voltammetry curves of the as-prepared FM-NS/NF electrode with various

Mn doping levels without iR-Corrected.
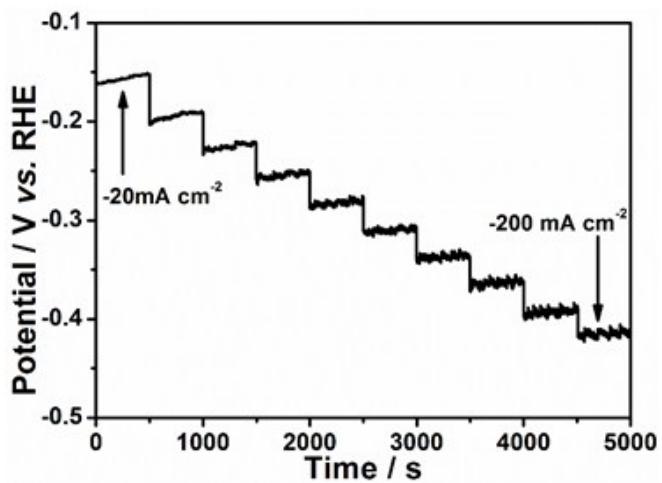
Fig. S29 Multicurrent process of the as-prepared NiFeMn-LTH/FM-NS/NF-4 electrode for HER.

The current density started at -20 mA cm^{-2} and ended at -200 mA cm^{-2}, with a decrement of 20

mA cm^{-2} per 500 s without iR correction.
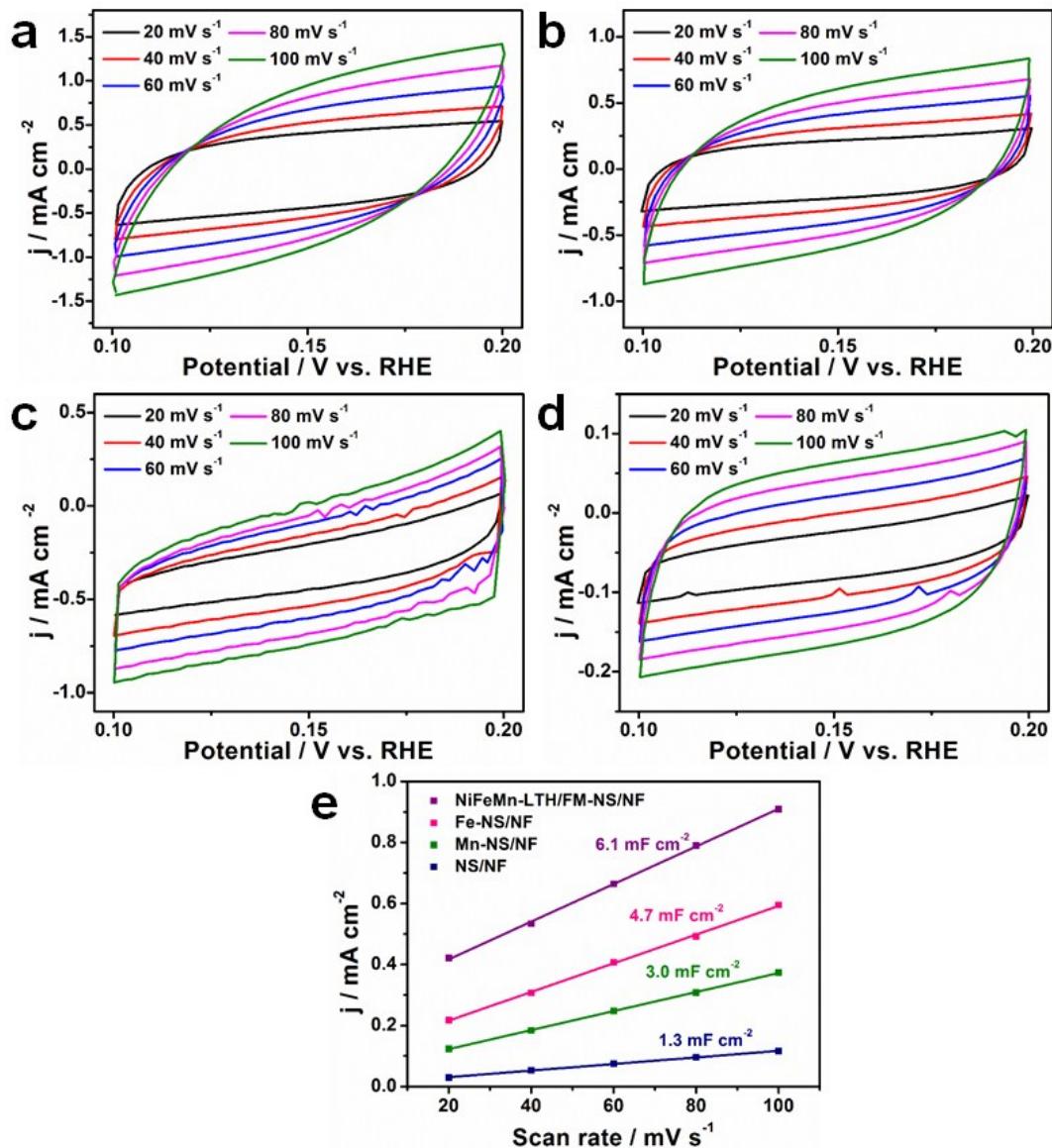
Fig. S30 Electrochemical double-layer capacitance measurements at different scan rate (20, 40, 60, 80, 100 mV s^{-1}) for HER in 1.0 M KOH. Cyclic voltammograms of the as-prepared (a) NiFeMn-LTH/FM-NS/NF, (b) Fe-NS/NF, (c) Mn-NS/NF, (d) NS/NF electrodes and (e) Charging current density plots with different scan rates for HER. The linear slope, equivalent to twice the double-layer capacitance (C$_{dl}$), was used to represent the ECSA.
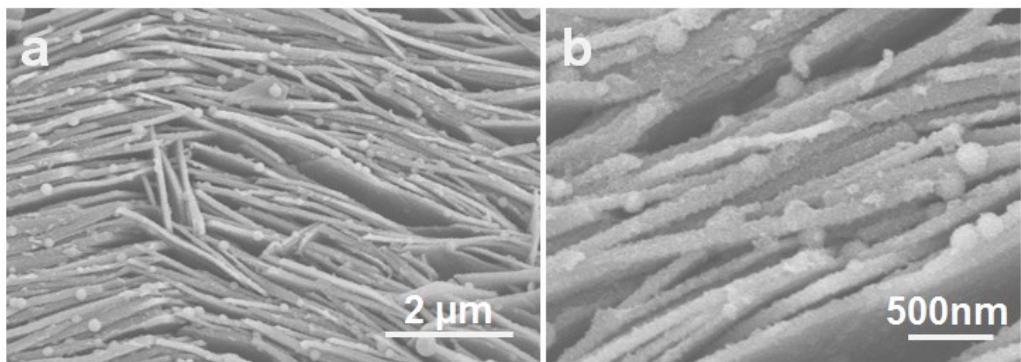
Fig. S31 SEM images of the NiFeMn-LTH/FM-NS/NF after the HER test.
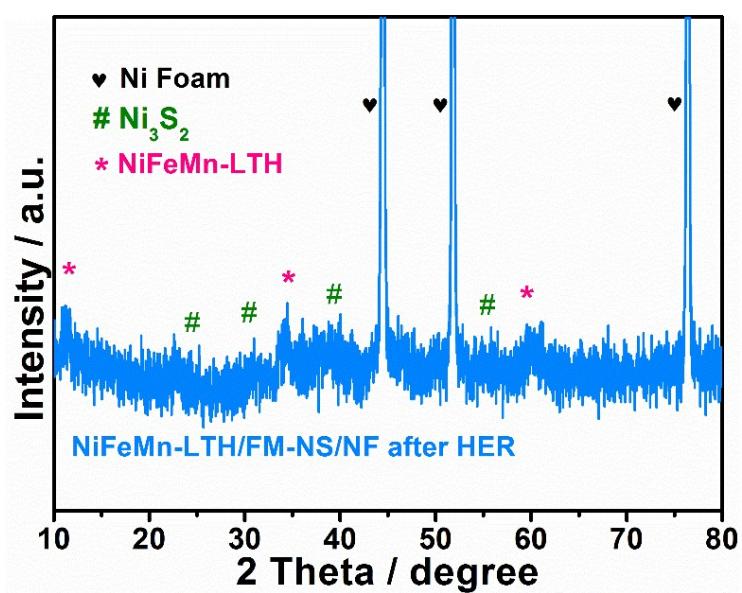
**Fig. S32** XRD pattern of the NiFeMn-LTH/FM-NS/NF-4 after the HER test.
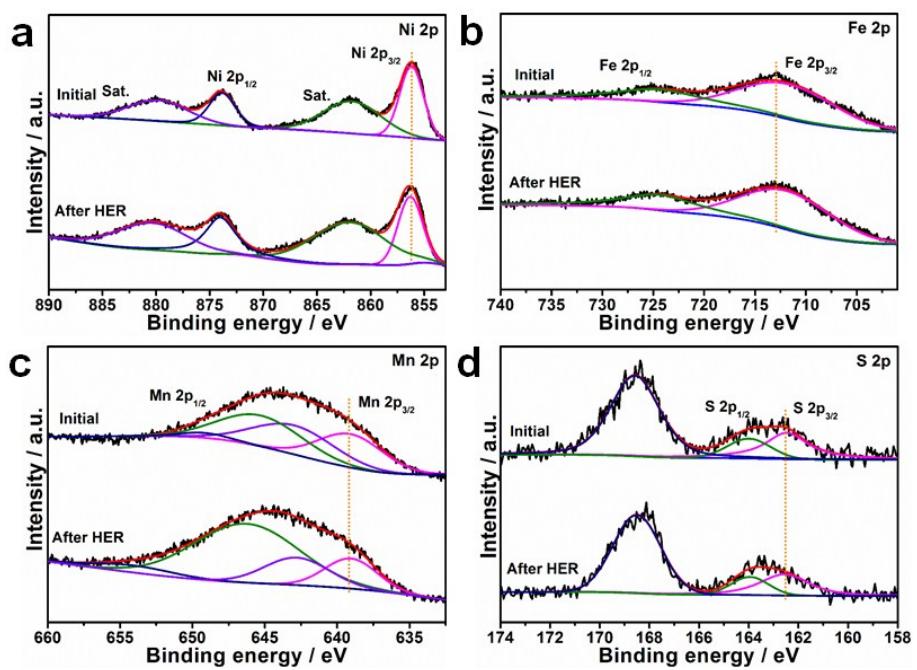
Fig. S33 XPS spectra of (a) Ni 2p, (b) Fe 2p, (c) Mn 2p and (d) S 2p of the as-prepared NiFeMn-

LTH/FM-NS/NF before and after HER test.
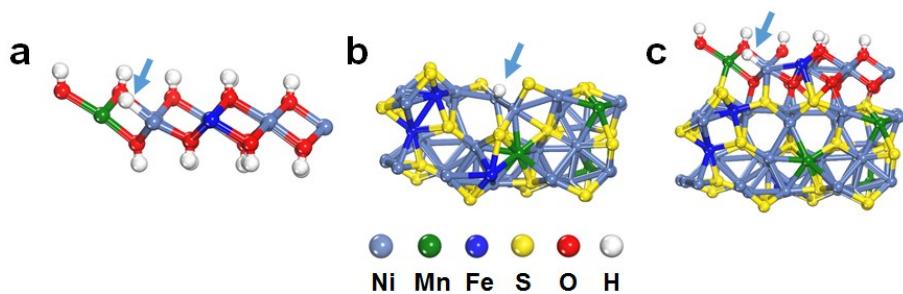
Fig. S34 The optimized structural representations for hydrogen adsorption at (a) NiFeMn-LTH, (b) FM-NS, and (c) NiFeMn-LTH/FM-NS.
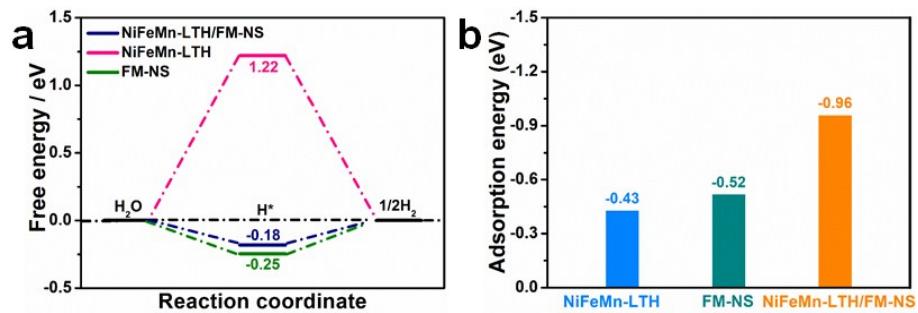
Fig. S35 (a) Gibbs free-energy diagram for H adsorption and (b) Adsorption energy for H_2O on the NiFeMn-LTH, FM-NS, and NiFeMn-LTH/FM-NS.

Table S1. Comparison of OER performances of as-prepared FM-NS/NF with other transition-metal catalysts in 1 M KOH solutions.

Catalysts	η_{10} / mV *vs.* RHE	Tafel slope / mV dec^{-1}	Ref.
FM-NS/NF	188	47	This work
$Fe_{0.09}Co_{0.13}$-NiSe$_2$/CFC	251	63	1
Fe-CoP HTPAs/NF	230	69	2
CoP-FeP/CC	250	131	3
$Cu_{0.3}Co_{2.7}$P/NC	190	44	4
Co/CoP	340	79.5	5
MoS$_2$/Ni$_3$S$_2$/NF	218	88	6
NiFeV LDHs/NF	195	42	7
Ni$_2$P-Ni$_3$S$_2$ HNAs/NF,	210	62	8
NiFe-LDH/NF	255	50	9
NiFeRu-LDH/NF	225	32	10

Table S2. Catalyst mass loading and Turnover frequency (TOF) of all used catalysts.

	Mass loading (mg cm^{-2})	TOF at η = 300 mV (s^{-1}) (OER)	TOF at η = -300 mV (s^{-1}) (HER)
FM-NS/NF	0.91	0.138	/
NFM-LTH/FM-NS/NF	0.93	/	0.30
Fe-NS/NF	1.01	0.042	0.082
Mn-NS/NF	1.08	0.003	0.053
NS/NF	1.15	0.002	0.021

Table S3. The corresponding EIS parameters for OER of the as-prepared FM-NS/NF, Fe-NS/NF,

Mn-NS/NF and NS/NF electrodes.

	FM-NS/NF	Fe-NS/NF	Mn-NS/NF	NS/NF
R_s (Ω cm^2)	1.01	1.07	1.08	1.20
R_{ct} (Ω cm^2)	2.27	92.2	67.3	354.5
CPE1-T	1.37	1.16	0.45	0.48
CPE1-P	0.66	0.41	0.61	0.67

Table S4. Comparison of HER performances of as-prepared NiFeMn-LTH/FM-NS/NF-4 with other transition-metal catalysts in 1 M KOH solutions.

Catalysts	η_{10} / mV *vs.* RHE	Tafel slope / mV dec^{-1}	Ref.
NiFeMn-LTH/FM-NS/NF-4	110	80	This work
NixCo$_{3-x}$S$_4$/Ni$_3$S$_2$/NF	160	95	11
Co$_1$–Fe$_1$–B–P	173	96	12
Mn-Ni$_3$S /NF	152	98	13
Co$_1$Mn$_1$CH/NF	180	/	14
Ni@N$_{0.19}$/NF	42	89	15
Ni$_3$S$_2$@NiV-LDH/NF	126	90	16
Cu3P–Co$_2$P /NF	115	65	17
NiCo$_2$S$_4$ NW/NF	210	59	18

Table S5. The corresponding EIS parameters for HER of the as-prepared NiFeMn-LTH/FM-NS/NF-4, Fe-NS/NF, Mn-NS/NF, NS/NF electrodes.

	NiFeMn-LTH/ FM-NS/NF-4	Fe-NS/NF	Mn-NS/NF	NS/NF
R_s (Ω cm^2)	1.02	1.03	1.21	1.04
R_{ct} (Ω cm^2)	2.89	3.83	8.23	14.12
CPE1-T	1.17	0.11	0.02	0.02
CPE1-P	2.93	0.67	0.72	0.71

Table S6. Overall water splitting performances of our samples compared with recently reported transition-metal catalysts in alkaline.

Catalysts	Potential (V) at 10 mA cm^{-2}	Ref.
FM-NS/NF // NiFeMn-LTH/FM-NS/NF-4	1.48	This work
$MoS_2/Ni_3S_2/NF$	1.56	6
$NixCo_{3-x}S_4/Ni_3S_2/NF$	1.53	9
$Ni_3S_2@NiV-LDH/NF$	1.53	16
CoMoNiS-NF-31	1.54	19
NiFe-LDH@NiCu	1.50	20
CoTeNR/NF	1.64	21
$Fe-Ni_3S_2/NF$	1.54	22
$Co_3S_4/EC-MOF/NF$	1.55	23

References

1.   Y. Sun, K. Xu, Z. Wei, H. Li, T. Zhang, X. Li, W. Cai, J. Ma, H. J. Fan and Y. Li, *Adv. Mater.*, 2018, **30**, e1802121.

2.   E. Hu, J. Ning, D. Zhao, C. Xu, Y. Lin, Y. Zhong, Z. Zhang, Y. Wang and Y. Hu, *Small*, 2018, **14**, e1704233.

3.   Z. Niu, C. Qiu, J. Jiang and L. Ai, *ACS Sustain. Chem. Eng.*, 2018, **7**, 2335-2342.

4.   J. Song, C. Zhu, B. Z. Xu, S. Fu, M. H. Engelhard, R. Ye, D. Du, S. P. Beckman and Y. Lin, *Adv. Energy Mater.*, 2017, **7**, 1601555.

5.   Z. H. Xue, H. Su, Q. Y. Yu, B. Zhang, H. H. Wang, X. H. Li and J. S. Chen, *Adv. Energy Mater.*, 2017, **7**, 1602355.

6.   J. Zhang, T. Wang, D. Pohl, B. Rellinghaus, R. Dong, S. Liu, X. Zhuang and X. Feng,

Angew. Chem. Int. Ed. Engl., 2016, **55**, 6702-6707.

7. P. S. Li, X. X. Duan, Y. Kuang, Y. P. Li, G. X. Zhang, W. Liu and X. M. Sun, *Adv. Energy Mater.*, 2018, **8**, 1703341.

8. L. Y. Zeng, K. A. Sun, X. B. Wang, Y. Q. Liu, Y. Pan, Z. Liu, D. W. Cao, Y. Song, S. H. Liu and C. G. Liu, *Nano Energy*, 2018, **51**, 26-36.

9. Z. Lu, W. Xu, W. Zhu, Q. Yang, X. Lei, J. Liu, Y. Li, X. Sun and X. Duan, *Chem. Commun.*, 2014, **50**, 6479-6482.

10. G. Chen, T. Wang, J. Zhang, P. Liu, H. Sun, X. Zhuang, M. Chen and X. Feng, *Adv. Mater.*, 2018, **30**, 1706279.

11. Y. Wu, Y. Liu, G.-D. Li, X. Zou, X. Lian, D. Wang, L. Sun, T. Asefa and X. Zou, *Nano Energy*, 2017, **35**, 161-170.

12. Z. Wu, D. Nie, M. Song, T. Jiao, G. Fu and X. Liu, *Nanoscale*, 2019, **11**, 7506-7512.

13. H. Du, R. Kong, F. Qu and L. Lu, *Chem. Commun.*, 2018, **54**, 10100-10103.

14. T. Tang, W. J. Jiang, S. Niu, N. Liu, H. Luo, Y. Y. Chen, S. F. Jin, F. Gao, L. J. Wan and J. S. Hu, *J. Am. Chem. Soc.*, 2017, **139**, 8320-8328.

15. Y. Li, X. Tan, S. Chen, X. Bo, H. Ren, S. C. Smith and C. Zhao, *Angew. Chem. Int. Ed. Engl.*, 2019, **58**, 461-466.

16. Q. Liu, J. Huang, Y. Zhao, L. Cao, K. Li, N. Zhang, D. Yang, L. Feng and L. Feng, *Nanoscale*, 2019, **11**, 8855-8863.

17. L. Liu, L. Ge, Y. Sun, B. Jiang, Y. Cheng, L. Xu, F. Liao, Z. Kang and M. Shao, *Nanoscale*, 2019, **11**, 6394-6400.

18. A. Sivanantham, P. Ganesan and S. Shanmugam, *Adv. Funct. Mater.*, 2016, **26**, 4661-4672.

19. Z. Yuan, J. Li, M. Yang, Z. Fang, J. Jian, D. Yu, X. Chen and L. Dai, *J. Am. Chem. Soc.*, 2019, **141**, 4972-4979.

20. Y. Zhou, Z. Wang, Z. Pan, L. Liu, J. Xi, X. Luo and Y. Shen, *Adv. Mater.*, 2019, **31**, e1806769.

21. L. Yang, H. Xu, H. Liu, D. Cheng and D. Cao, *Small Methods*, 2019, **3**, 1900113.

22. G. Zhang, Y. S. Feng, W. T. Lu, D. He, C. Y. Wang, Y. K. Li, X. Y. Wang and F. F. Cao,

ACS Catal., 2018, **8**, 5431.

23.   T. Liu, P. Li, N. Yao, T. Kong, G. Cheng, S. Chen and W. Luo, *Adv. Mater.*, 2019, **31**, e1806672.